

Variability of signal to noise ratio and the network analysis of gravitational wave burst signals

Soumya D. Mohanty,^{1,*} Malik Rakhmanov,^{2,†} Sergei Klimenko,² and Guenakh Mitselmakher²

¹The University of Texas at Brownsville, 80 Fort Brown, Brownsville, Texas, 78520, USA

²University of Florida, P.O.Box 118440, Gainesville, Florida, 32611, USA

The detection and estimation of gravitational wave burst signals, with *a priori* unknown polarization waveforms, requires the use of data from a network of detectors. For determining how the data from such a network should be combined, approaches based on the maximum likelihood principle have proven to be useful. The most straightforward among these uses the global maximum of the likelihood over the space of all waveforms as both the detection statistic and signal estimator. However, in the case of burst signals, a physically counterintuitive situation results: for two aligned detectors the statistic includes the cross-correlation of the detector outputs, as expected, but this term disappears even for an infinitesimal misalignment. This *two detector paradox* arises from the inclusion of improbable waveforms in the solution space of maximization. Such waveforms produce widely different responses in detectors that are closely aligned. We show that by penalizing waveforms that exhibit large signal-to-noise ratio (snr) variability, as the corresponding source is moved on the sky, a physically motivated restriction is obtained that (i) resolves the two detector paradox and (ii) leads to a better performing statistic than the global maximum of the likelihood. Waveforms with high snr variability turn out to be precisely the ones that are improbable in the sense mentioned above. The coherent network analysis method thus obtained can be applied to any network, irrespective of the number or the mutual alignment of detectors.

I. INTRODUCTION

Several interferometric gravitational wave (GW) detectors are now operational around the world [1, 2, 3, 4] in addition to an already operating set of resonant mass detectors [5]. Since gravitational wave detectors can measure both the amplitude and phase of incoming signals, it is possible to combine the data from such a network of detectors to not only detect GW sources better, compared to single detectors, but also estimate the waveforms of the two independent polarization components of the GW signal along with the direction to the source.

A straightforward approach to signal detection and estimation using data from a network of detectors is through the likelihood [6] functional. The likelihood functional of data \mathbf{x} is the joint probability density function $p(\mathbf{x}|\theta)$, where θ is a vector of parameters whose true value for any given instance of \mathbf{x} is not known *a priori*. In the case of GW detection, \mathbf{x} is the collection of outputs from all the detectors in a network and the parameters are the sky position of the GW source and the waveforms of the two GW polarization components, $h_+(t)$ and $h_\times(t)$. The problem of signal detection is concerned with deciding whether \mathbf{x} is a realization of $p(\mathbf{x}|\theta_0)$ or $p(\mathbf{x}|\theta \neq \theta_0)$, where θ_0 denotes the signal absent case. The estimation problem deals with inferring the true value of θ once a detection has been made. According to the maximum likelihood [6] approach to inference, the value θ_{\max} at which the likelihood functional attains its maximum

serves as an estimate of the true value of θ . The maximum, over θ , of the likelihood ratio (LR) functional $p(\mathbf{x}|\theta)/p(\mathbf{x}|\theta_0)$ yields a detection statistic. Thus, the likelihood based approach conveniently yields both a detection statistic and source parameter estimates.

For binary inspiral signals, the polarization waveforms can be computed in terms of a small set of parameters describing the binary, such as the masses of the two stars, the orbital inclination etc. Likelihood based network analysis is fairly well understood in the case of such known waveforms [7, 8]. In this paper, we consider likelihood based network analysis for burst signals that are short duration deterministic signals but have unreliable or simply unknown waveforms. Astrophysical sources of burst signals include Supernovae [9], Gamma Ray Bursts [10] and the merger of compact objects such as Neutron stars and Black Holes [11].

Although we do not have prior knowledge of burst signal waveforms, it is possible to extend likelihood based network analysis to burst signals in a formal sense. The basic idea [12, 13, 14, 15] is to treat each sample of a burst signal as a parameter and maximize the likelihood over all the parameters. We refer to the resulting detection method as standard likelihood (SL). Other approaches to network analysis for burst signals have also been proposed in the literature [16, 17]. The method [16] proposed by Gürsel and Tinto is based on extremizing a functional that is constructed purely out of the response of each detector in a network and does not explicitly depend on the polarization waveforms. A minimum of three misaligned detectors are required in order to use the Gürsel-Tinto method whereas likelihood based methods do not have this limitation.

Although it is quite elegant, the SL method has a fundamental problem that was first noted in [14] and system-

*Electronic address: mohanty@phys.utb.edu

†Currently at: Department of Physics, Pennsylvania State University, University Park, PA 16802, USA

atically analyzed in [15] (henceforth, KMRM). Called the two detector paradox, the problem is most easily stated for a network of two detectors. When the detectors are perfectly aligned, the SL detection statistic naturally includes the cross-correlation of detector outputs. Since the response to a given GW source is identical in aligned detectors, this term serves to increase the sensitivity of the overall detection statistic. However, it disappears when the SL approach is used for even infinitesimally misaligned detectors. This is counterintuitive since we expect the cross-correlation term to remain important for small misalignments.

The origin of the two detector paradox is that all waveforms for $h_+(t)$ and $h_\times(t)$ are allowed as solutions when maximizing the likelihood even though some of them would be improbable in that they will produce widely different responses in two nearly aligned detectors. It follows that this problem can be solved by removing such improbable waveforms from the space of allowed solutions. In KMRM, this was achieved by imposing certain constraints on the space of waveforms yielding the class of constraint likelihood methods. Modifying the likelihood functional with a waveform dependent weight factor, such as a Bayesian prior [18], is another way of suppressing undesirable solutions. In the following we use the term “restriction” to encompass all approaches that remove improbable solutions or reduce their influence.

The non-trivial aspect of setting up restrictions is that the performance of the resulting statistic must not be degraded and, if possible, should be better than the SL approach. Additionally, the restrictions must be applicable to all astrophysical burst sources otherwise the resulting statistic will be better for a particular type of source but may be worse for others. If sufficiently reliable knowledge for a particular class is available, then it can be used [19, 20] as an additional set of restrictions to further enhance sensitivity. The constraints proposed in KMRM (see Section III) satisfy the above condition, namely independence from assumptions about source dynamics. Simulations show that constraint likelihood methods perform significantly better than SL, especially in reconstructing the sky position of a burst source. However, the constraints used were a first example and are not necessarily unique or optimal. It is important to investigate independent avenues of formulating generic restrictions in order to gain more insight into this promising approach to network analysis.

We investigate the issue of generic restrictions from a physical point of view. It is found that the more improbable a set of waveforms h_+ and h_\times , the faster is the change in detectability of the corresponding source as a function of sky position. By measuring the rate of change of signal-to-noise ratio (SNR) as a function of sky position, therefore, we can restrict solutions that are undesirable in the maximization of the LR. Monte Carlo simulations show that the detection statistic that results from the above restriction performs roughly the same as constraint likelihood methods. However, there exist im-

portant qualitative differences in how the two methods process data. For example, unlike constraint likelihood, the divergence from SL of the method introduced here depends on the actual data.

The paper is organized as follows. We review the standard likelihood method in Section II, establishing our basic notation and conventions on the way. Section III contains a discussion of the two detector paradox. Section IV considers the SNR variability of signals, discusses how it affects their detectability and defines a measure for it. Section V contains the derivation of the detection statistic and source parameter estimators that result from incorporating SNR variability. Results from simulations are presented in Section VI.

II. STANDARD LIKELIHOOD ANALYSIS FOR BURST SIGNALS

We fix a Cartesian coordinate system with its origin at the center of the Earth, Z axis pointing at the North Pole and some arbitrary convention for the X and Y axes. This will be our fiducial frame of reference. Let the sky position of an incoming GW signal in this frame be denoted by θ , the polar angle, and ϕ , the azimuthal angle. An incoming GW signal is most conveniently expressed in the transverse traceless (TT) gauge [21] associated with the source direction. The Z axis of the TT frame is oriented along the direction to the GW source. We adopt the convention that the X axis of the TT gauge lies in the plane formed by the TT frame Z axis and the Z axis of the fiducial frame. The GW signal is specified by its two independent polarization components $h_+(t)$ and $h_\times(t)$ in the TT frame.

In this paper, we take into account the different orientations and geographic locations of currently operating interferometric detectors but treat them as identical in sensitivity. For instance, a GEO detector in the paper will mean a detector having the same location and orientation as GEO600 but with sensitivity similar to that of LIGO detectors. This simplifies the algebra considerably without altering the main result which is the relative comparison of methods.

Since real data is digital, we shift to the discrete time domain and from here on denote any time dependent quantity $g(t)$ as $g[j]$, where $t = j\delta$, δ being the sampling interval. A finite sequence of time samples $\{g[0], g[1], \dots, g[m-1]\}$ will be denoted by \bar{g} . The scalar response of a detector $s[k]$ to an incoming GW is given by,

$$s[k] = W^{ij}[k]D_{ij}, \quad (1)$$

where W^{ij} is the symmetric trace free tensor that describes the GW in the transverse-traceless gauge and D_{ij} is an equivalent tensor associated with the detector [22]. (The Einstein summation convention is in force in the above expression.) The response $s_i[k]$ of the i^{th} detector,

$i = 1, \dots, N_d$, is expressed as,

$$s_i[k] = F_{+,i}(\theta, \phi)h_{+}[k\delta - \delta_i] + F_{\times,i}(\theta, \phi)h_{\times}[k\delta - \delta_i], \quad (2)$$

where $F_{+,i}$ and $F_{\times,i}$ depend on the rotations involved in going from the TT frame associated with a detector to the wave frame associated with the fiducial frame and δ_i is the travel time for the signal from the origin of the fiducial frame to the detector. For a given θ, ϕ , we can treat the detectors as co-located ($\delta_i = 0$) at the origin of the fiducial frame since the output from each detector can be shifted in time to compensate for δ_i .

For a network of detectors, it is convenient to define quantities that are analogous to those for a single detector. Thus, we can define a network response vector,

$$\mathbf{S}[k] = \begin{pmatrix} s_1[k] \\ \vdots \\ s_{N_d}[k] \end{pmatrix}. \quad (3)$$

Vectors in \mathbb{R}^{N_d} , the space of real N_d -tuples, will be denoted by boldface capital letters. By convention, every vector $\mathbf{A} \in \mathbb{R}^{N_d}$ will be a column vector. We define the Euclidean scalar product in this space, $\mathbf{A} \cdot \mathbf{B} = \mathbf{A}^T \mathbf{B}$. A sequence of vectors will be denoted by $\overline{\mathbf{A}} = \{\mathbf{A}[0], \dots, \mathbf{A}[m-1]\}$.

For given θ, ϕ ,

$$\mathbf{S}[k] = \mathcal{F}(\theta, \phi) \begin{pmatrix} h_{+}[k] \\ h_{\times}[k] \end{pmatrix}, \quad (4)$$

where the matrix \mathcal{F} is defined as,

$$\mathcal{F}(\theta, \phi) = \begin{pmatrix} F_{+,1}(\theta, \phi) & F_{\times,1}(\theta, \phi) \\ \vdots & \vdots \\ F_{+,N_d}(\theta, \phi) & F_{\times,N_d}(\theta, \phi) \end{pmatrix}. \quad (5)$$

Given a network response vector $\mathbf{S}[k]$, the polarization components can be obtained as,

$$\begin{pmatrix} h_{+}[k] \\ h_{\times}[k] \end{pmatrix} = \mathcal{H}^{-1} \mathcal{F}^T(\theta, \phi) \mathbf{S}[k], \quad (6)$$

$$\mathcal{H}(\theta, \phi) = \mathcal{F}^T(\theta, \phi) \mathcal{F}(\theta, \phi), \quad (7)$$

provided \mathcal{H}^{-1} exists. (Note that \mathcal{H} is a symmetric 2-by-2 matrix and, hence, has two real eigenvalues.)

Let the noise in the i^{th} detector be \bar{n}_i . In the following we will assume that \bar{n}_i is a zero mean, white, Gaussian process, i.e., $E[n_i[j]] = 0$ and $E[n_i[j]n_m[k]] = \delta_{im}\delta_{jk}$. In analogy to the network response vector $\mathbf{S}[k]$, we define a network data vector $\mathbf{X}[k]$,

$$\mathbf{X}[k] = \begin{pmatrix} x_1[k] \\ \vdots \\ x_{N_d}[k] \end{pmatrix} = \begin{pmatrix} n_1[k] \\ \vdots \\ n_{N_d}[k] \end{pmatrix} + \mathbf{S}[k]. \quad (8)$$

The natural logarithm of the likelihood ratio (LR), $\Lambda(\overline{\mathbf{X}}|\theta, \phi, \overline{\mathbf{S}})$, for an N_d detector network is given by

$$\begin{aligned} \Lambda(\overline{\mathbf{X}}|\theta, \phi, \overline{\mathbf{S}}) &= \frac{1}{2} \sum_{i=1}^{N_d} \sum_{j=0}^{N-1} (x_i[j]^2 - (x_i[j] - s_i[j])^2) \quad (9) \\ &= \sum_{j=0}^{N-1} \left[\mathbf{X}[j] \cdot \mathbf{S}[j] - \frac{1}{2} \|\mathbf{S}[j]\|^2 \right], \quad (10) \end{aligned}$$

where the detectors outputs are implicitly time shifted as explained above.

The maximum likelihood ratio approach can be extended to burst signals by substituting Eq. 4 into Eq. 10 and maximizing $\Lambda(\overline{\mathbf{X}}|\theta, \phi, \overline{\mathbf{S}})$ over each $h_{+}[j]$, $h_{\times}[j]$ independently. Since the resulting equations involve only quantities at the same sample j , this involves maximizing the summand in Eq. 10 independently for each j . From now onwards we will focus on only one time instant and drop the time index when there is no scope for confusion. The quantity to be maximized is,

$$\lambda[j] = \mathbf{X}[j] \cdot \mathbf{S}[j] - \frac{1}{2} \|\mathbf{S}[j]\|^2, \quad (11)$$

over the vector \mathbf{S} in \mathbb{R}^{N_d} , the space of real N_d -tuples. Let the maximum of λ occur at \mathbf{S}_{max} . If the maximization allows all possible \mathbf{S} , then it is obvious that $\mathbf{S}_{max} = \mathbf{X}$. However, we are not allowed to choose any arbitrary \mathbf{S} in the evaluation of λ since from Eq. 4, \mathbf{S} is a vector that depends on only two parameters $h_{+}[j]$ and $h_{\times}[j]$. This implies that \mathbf{S} must lie in a two dimensional plane determined completely by the antenna pattern functions of the detectors and passing through the origin of \mathbb{R}^{N_d} .

Though the maximization of λ is restricted to \mathbf{S} lying in the response plane, in the maximum likelihood ratio approach there are no further constraints on the choice of \mathbf{S} within this plane. We call the method of maximizing λ over \mathbf{S} with no further restrictions as the standard likelihood (SL) method [11, 13, 14, 15, 19]. We denote the value of Λ (Eq. 10), obtained by summing the maximized values of λ corresponding to each time instant, by $\Lambda_{SL}(\theta, \phi)$. This is the detection statistic of the SL method.

III. THE TWO DETECTOR PARADOX

In the two detector case, the network data vector \mathbf{X} lies in the response plane. When the detectors are aligned, we are constrained to use a network response vector \mathbf{S} lying along the 45° line since the responses of the two detectors must be identical, $s_1[k] = s_2[k] = s[k]$ for all k . Maximizing λ over the response $s[k]$ yields,

$$\hat{s} = \frac{1}{2}(x_1 + x_2), \quad (12)$$

$$\hat{\lambda} \propto \frac{1}{2}(x_1 + x_2)^2, \quad (13)$$

where $\widehat{\lambda}$ denotes the maximum value and $\widehat{\lambda} = \lambda(\widehat{\mathbf{s}})$. It follows that,

$$\Lambda_{SL}(\theta, \phi) \propto \sum_{j=0}^{N-1} (x_1[j]^2 + x_2[j]^2 + 2x_1[j]x_2[j]) . \quad (14)$$

Thus, the SL detection statistic contains a cross-correlation term, $\sum x_1[j]x_2[j]$, which agrees with our intuition: since the responses of the two detectors are identical, the cross-correlation term will always have a positive definite mean in the presence of a signal and, therefore, should be useful for detection.

However, the same procedure, when carried out for even infinitesimally misaligned detectors, yields Λ_{SL} that has no cross-correlation term,

$$\widehat{s}_1 = x_1 \quad ; \quad \widehat{s}_2 = x_2 , \quad (15)$$

$$\widehat{\lambda} \propto x_1^2 + x_2^2 . \quad (16)$$

This clearly violates what one expects on physical grounds since the cross-correlation term should remain a useful discriminant against noise when the detectors are only infinitesimally misaligned. However, for the class of probable waveforms, the SL statistic becomes less sensitive than one in which a cross-correlation term is added by hand. Thus, the SL approach fails to deliver a physically acceptable detection statistic in the two detector case. Following KMRM we call this problem the two detector paradox.

The origin of the two detector paradox lies in the maximization of λ over all waveforms, h_+ and h_\times , including those that can produce very different responses s_1 and s_2 for even infinitesimally misaligned detectors. Such waveforms can lead to small or even zero cross-correlation between the responses. Physical intuition suggests that such waveforms should be improbable. Mathematically, however, such waveforms are allowed since the matrix \mathcal{F} is invertible, even if it is nearly singular, and some h_+ and h_\times can always be obtained for any given s_1 and s_2 . As a result, the SL approach “throws” out the cross-correlation term since this term can now contribute pure noise. Geometrically, the two detector paradox comes about because the data vector \mathbf{X} lies in the response plane and the SL approach does not constrain the choice of \mathbf{S} in this plane. Hence, the solution $\widehat{\mathbf{S}} = \mathbf{X}$ that removes cross-correlation is an allowed one in this case. This suggests that restricting the allowed solutions in the response plane can resolve the two detector paradox. The SL detection statistic recovers pair-wise cross-correlations in the case of three or more misaligned detectors since \mathbf{X} now lies outside the response plane. However, the two detector paradox is just an extreme manifestation of a problem that occurs for any arbitrary network: depending on the geometry of the network, some solutions are improbable and their inclusion in the maximization of the LR reduces its sensitivity.

IV. VARIABILITY OF SNR OVER THE SKY

Though our physical intuition suggests that an infinitesimal misalignment between two detectors should not result in very different responses $s_1 \simeq s_2$, this does not forbid the existence of such sources. As discussed above, mathematically, $h_+(t)$ and $h_\times(t)$ can be completely arbitrary and, in particular, can be such that s_1 is very different from s_2 . However, we expect such sources to be improbable. Is their a quantitative basis for our expectation? In this section we show that, indeed, there is a natural argument that “probable” GW sources, for which $s_1 \simeq s_2$, should occur more often than “improbable” ones. Note that the categorization of a source as probable or improbable also depends on the mutual alignment of detectors. For example, two detectors oriented at 45° to each other can often have very different responses for the same source. As shown below, our argument takes this factor into account. We first present the two detector case and then consider an arbitrary network.

A. Two detector case

Consider a gravitational wave source located at (θ, ϕ) with signal polarization components $h_+[k]$ and $h_\times[k]$. Let the detector response vector be $\mathbf{S}[k]$. Now consider an identical source located at (θ', ϕ') . By this we mean that the fiducial frame, along with the GW source, be rotated rigidly leaving the detectors in their original place. This leads to a network response $\mathbf{S}'[k]$ that is related to $\mathbf{S}[k]$ by,

$$\mathbf{S}' = \mathcal{F}(\theta', \phi')\mathcal{F}^{-1}(\theta, \phi)\mathbf{S} . \quad (17)$$

Now, assume that we use matched filtering [23] to detect the source at the instant k . Thus, our detection statistic will be $\mathbf{X}[k] \cdot \mathbf{S}[k]$ and $\mathbf{X}[k] \cdot \mathbf{S}'[k]$ for the two sources respectively. The detectability of a source under matched filtering is measured by the signal to noise ratio (SNR), ρ , defined as the ratio of the mean of the detection statistic to its standard deviation. For the two sources above, the respective SNR will be $\rho = \|\mathbf{S}[k]\|$ and $\rho' = \|\mathbf{S}'[k]\|$. Note that we are considering a more restricted version of matched filtering than the conventional one in which the detection statistic would be $\sum \mathbf{X}[k] \cdot \mathbf{S}[k]$ and the SNR would be $\rho^2 = \sum \|\mathbf{S}[k]\|^2$. We return to this point later in this section.

We denote the relative difference in SNR for the two source locations as,

$$\epsilon(\theta, \phi, \theta', \phi'; \widehat{S}) = \frac{\rho' - \rho}{\rho} , \quad (18)$$

where \widehat{S} is the unit vector oriented along \mathbf{S} . For small

displacements, $\theta' = \theta + \delta\theta$ and $\phi' = \phi + \delta\phi$, we get,

$$\epsilon(\theta, \phi, \theta', \phi'; \hat{S}) = \delta\theta \left. \frac{\partial \epsilon}{\partial \theta'} \right|_{\substack{\theta'=\theta, \\ \phi'=\phi}} + \delta\phi \left. \frac{\partial \epsilon}{\partial \phi'} \right|_{\substack{\theta'=\theta, \\ \phi'=\phi}}, \quad (19)$$

$$\begin{aligned} \left. \frac{\partial \epsilon}{\partial \theta'} \right|_{\substack{\theta'=\theta, \\ \phi'=\phi}} &= \frac{\partial}{\partial \theta'} \sqrt{\|\mathcal{F}(\theta', \phi') \mathcal{F}^{-1}(\theta, \phi) \hat{S}\|^2} \Big|_{\substack{\theta'=\theta, \\ \phi'=\phi}}, \\ &= \hat{S} \cdot \left(\frac{\partial \mathcal{F}(\theta, \phi)}{\partial \theta} \mathcal{F}^{-1}(\theta, \phi) \hat{S} \right), \\ \left. \frac{\partial \epsilon}{\partial \phi'} \right|_{\substack{\theta'=\theta, \\ \phi'=\phi}} &= \hat{S} \cdot \left(\frac{\partial \mathcal{F}(\theta, \phi)}{\partial \phi} \mathcal{F}^{-1}(\theta, \phi) \hat{S} \right). \end{aligned} \quad (20)$$

The norm of the gradient

$$\mathcal{G}(\theta, \phi; \hat{S}) = \left[\left(\hat{S} \cdot \left(\mathcal{F}_\theta \mathcal{F}^{-1} \hat{S} \right) \right)^2 + \left(\hat{S} \cdot \left(\mathcal{F}_\phi \mathcal{F}^{-1} \hat{S} \right) \right)^2 \right]^{1/2}, \quad (21)$$

$\mathcal{F}_\theta = \partial \mathcal{F} / \partial \theta$ and $\mathcal{F}_\phi = \partial \mathcal{F} / \partial \phi$, is a convenient measure of the variability of the SNR of a source as a function of its location.

A high value of $\mathcal{G}(\theta, \phi; \hat{S})$ implies that the source would have to occur at very special positions on the sky to be detectable. This is because if it has an SNR above some detection threshold at one location, it may rapidly fall below it if it were to occur at a slightly different location. Consider two classes of sources, class A with a large associated $\mathcal{G}(\theta, \phi; \hat{S})$ and class B with low values of the same. Assume that events from both classes occur with the same comoving rate and that they have the same distribution on the sky. Then, due to the rapid fluctuation of the SNR for source class A, the area of the sky over which its members will be detectable would be significantly less than that of class B. It follows that the observed rate of the class A sources would be much reduced in comparison to class B. Therefore, even though the two sources may be equivalent in terms of, say, the energy emitted in GWs, the high SNR variability source would be detectable less often. Since a larger volume of space would be required to detect such sources, it will naturally be harder to detect at a given false alarm rate.

We thus arrive at the main point of this section. Given a pair of misaligned detectors, we should include only those responses \mathbf{S} in our search for the maximum of the LR for which $\mathcal{G}(\theta, \phi; \hat{S})$ is low in some well defined sense. In this way, the detectability of sources with an intrinsically low observable rate will be reduced but that of more frequently observable sources will be enhanced. It is important to note that the above argument does not require any prior assumptions about the astrophysics of sources. Also note that \mathcal{G} depends only on the orientation of \mathbf{S} and not its magnitude. That is, it is only concerned with the shape of the waveforms of h_+ and h_\times and not the distance to the source.

Figure 1 shows polar plots of $\mathcal{G}(\theta, \phi; \hat{S})$ as a function of \hat{S} for fixed θ, ϕ and different detector alignments. It

is assumed that the detectors are colocated at the origin of the fiducial frame and coplanar with angles between their respective X arms of α . The antenna patterns are, in this case,

$$\mathcal{F} = \begin{pmatrix} \frac{1}{2}(1 + \cos^2 \theta) \cos 2\phi & \cos \theta \sin 2\phi \\ \frac{1}{2}(1 + \cos^2 \theta) \cos 2(\phi + \alpha) & \cos \theta \sin 2(\phi + \alpha) \end{pmatrix}. \quad (22)$$

Each plot is over all orientations of the detector response vector \hat{S} . First, we see that for almost coaligned detectors, $\alpha = 0.1^\circ$, if we limit the search for the maximum of λ (c.f., Eq. 11) over \hat{S} such that $\mathcal{G}(\theta, \phi; \hat{S}) \leq 10$, say, then only detector responses with orientation very close to the 45° and -45° line will be allowed. This means that the instantaneous response in the two detectors should be nearly equal. From this example, we see that waveforms with low SNR variability are also the ones that lead to nearly identical responses in the two detectors and, as discussed above, are the ones which have relatively higher chances of being detected. This bears out our physical intuition that sources that produce very different responses in nearly aligned detectors should be rare. As α is increased, one sees that not only does \mathcal{G} decrease but that it also approaches the same value for all orientation and, hence, all orientations of \hat{S} are now allowed. The pattern opens up fully when the detectors are at 45° to each other. As α approaches 90° , the responses are again increasingly restricted around the $\pm 45^\circ$ lines.

Though Fig. 1 shows that SNR variability is a natural measure for restricting the orientation of \hat{S} , the particular measure $\mathcal{G}(\theta, \phi; \hat{S})$ allows both $\pm 45^\circ$ lines as the locii of restriction. For nearly aligned detectors, however, we expect detector responses to be in-phase which means that the responses should lie in the vicinity of the $+45^\circ$ line. We introduce another function, $\Gamma(\theta, \phi; \hat{S})$, that is also a measure of SNR variability but has better properties in this respect.

$$\Gamma^2(\theta, \phi; \hat{S}) = \left\| \mathcal{F}_\theta \mathcal{F}^{-1} \hat{S} \right\|^2 + \left\| \mathcal{F}_\phi \mathcal{F}^{-1} \hat{S} \right\|^2, \quad (23)$$

In fact, from the Cauchy Schwartz inequality, it follows that

$$\mathcal{G}(\theta, \phi; \hat{S}) \leq \Gamma(\theta, \phi; \hat{S}). \quad (24)$$

Hence, $\Gamma(\theta, \phi; \hat{S})$ is an upper bound on SNR variability. Figure 2 shows polar plots of $\Gamma(\theta, \phi; \hat{S})$ for fixed θ, ϕ and different misalignment angles α . Now, for small misalignment ($\alpha = 0.1^\circ$), one sees that only responses along the $+45^\circ$ line are allowed while for misalignment close to 90° , only responses that are close to -45° are allowed. It makes sense, therefore, to use $\Gamma(\theta, \phi; \hat{S})$ as a measure of SNR variability instead of $\mathcal{G}(\theta, \phi; \hat{S})$.

In the above discussion, we considered the detection of a signal at a single instant using a matched filter, leading to the detection statistic $\mathbf{X}[k] \cdot \mathbf{S}[k]$. Burst signals can last

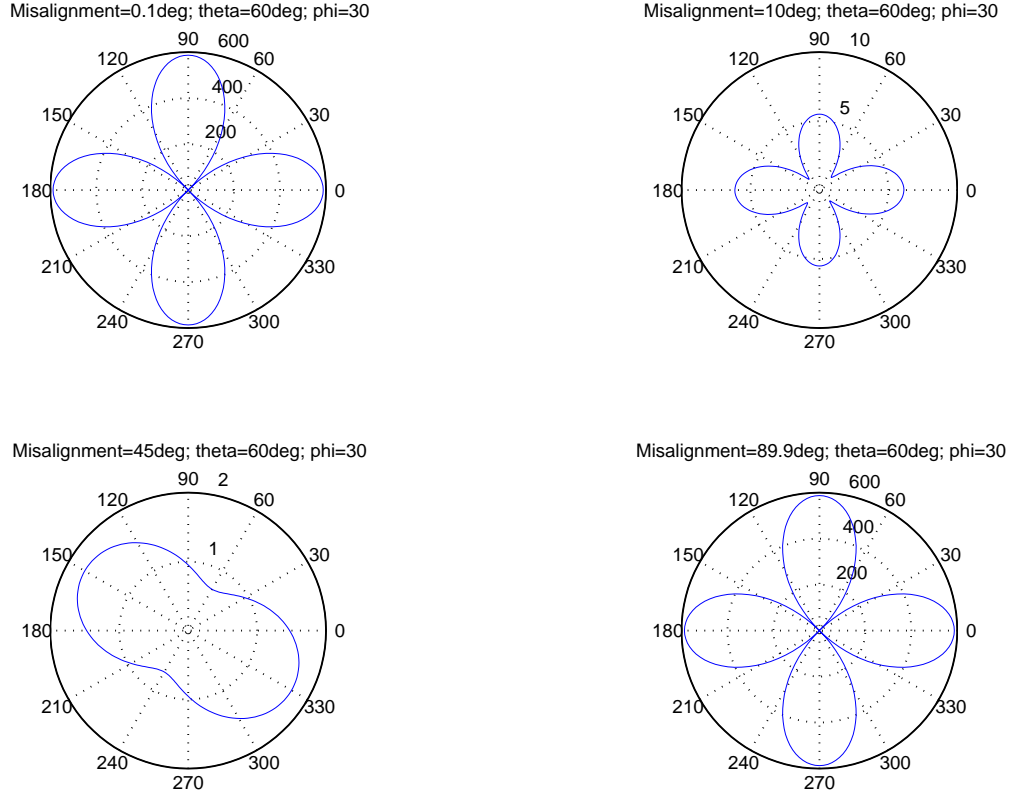


FIG. 1: Plots of \mathcal{G} (Eq. 21) for different misalignment angles.

over several sampling intervals and, in general, the detection statistic would in fact be a sum $\sum \mathbf{X}[k] \cdot \mathbf{S}[k]$ over a range of k . In this case, a high SNR variability response $\mathbf{S}[k]$ can be balanced by a very low variability response $\mathbf{S}[k']$ at some other instant, thus leading to a low variability for the overall SNR $= [\sum \|\mathbf{S}\|^2]^{1/2}$. This would allow a broader range of signals to be used for maximizing the overall likelihood Λ (c.f., Eq. 10). Our choice of using instantaneous SNR variability is simply a conservative one since signals with low instantaneous SNR variability will necessarily have low variability of their overall SNR. Moreover, as discussed earlier, physical intuition suggests that the responses in closely aligned detectors should be nearly identical at each instant of time and not just on the average.

B. General network of detectors

We will now generalize the SNR variability measure $\Gamma(\theta, \phi; \hat{S})$, introduced in Eq. 23, to the case of an arbitrary network of detectors. The relative difference in the observed SNR of the same source between two positions

(θ, ϕ) and (θ', ϕ') is,

$$\epsilon(\theta, \phi, \theta', \phi'; \hat{S}) = \|\mathcal{F}(\theta', \phi')\mathcal{H}^{-1}(\theta, \phi)\mathcal{F}^T(\theta, \phi)\hat{S}\| - 1. \quad (25)$$

As before, for a small displacement of the source,

$$\left. \frac{\partial \epsilon}{\partial \theta'} \right|_{\substack{\theta'=\theta \\ \phi'=\phi}} = \hat{S} \cdot (\mathcal{F}_\theta \mathcal{H}^{-1} \mathcal{F}^T \hat{S}), \quad (26)$$

$$\left. \frac{\partial \epsilon}{\partial \phi'} \right|_{\substack{\theta'=\theta \\ \phi'=\phi}} = \hat{S} \cdot (\mathcal{F}_\phi \mathcal{H}^{-1} \mathcal{F}^T \hat{S}), \quad (27)$$

and our measure of SNR variability will be defined as,

$$\Gamma^2(\theta, \phi; \hat{S}) = \left\| \mathcal{F}_\theta \mathcal{H}^{-1} \mathcal{F}^T \hat{S} \right\|^2 + \left\| \mathcal{F}_\phi \mathcal{H}^{-1} \mathcal{F}^T \hat{S} \right\|^2 \quad (28)$$

Here, \hat{S} is a unit vector in the R^{N_d} space but lying in the response plane.

For algebraic simplicity, it is convenient to express the response vector \mathbf{S} in terms of a basis in the response plane rather than the full R^{N_d} space. In order to do so, we need to fix two orthonormal vectors \hat{q}_0 and \hat{q}_1 on this plane. If \hat{e}_0 and \hat{e}_1 are the two orthonormal eigenvectors of \mathcal{H} ,

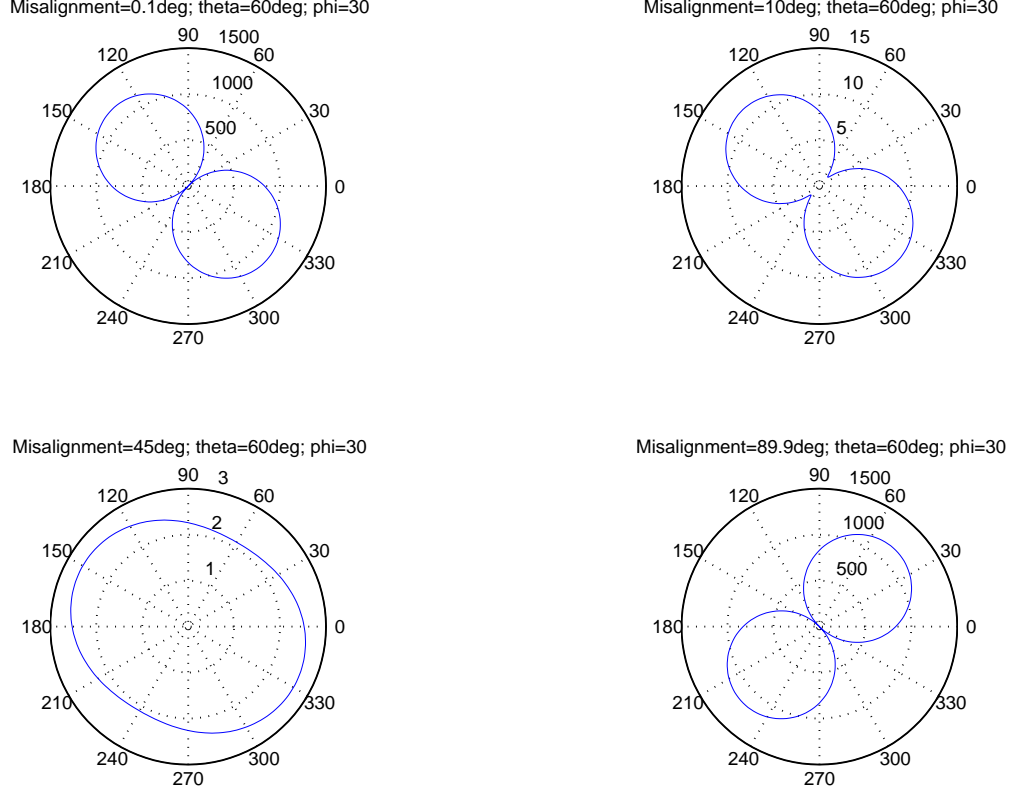


FIG. 2: Plots of Γ (Eq. 23) for different misalignment angles.

corresponding to eigenvalues ν_0 and ν_1 respectively, then it is easily seen that for,

$$\hat{q}_0 = \frac{1}{\sqrt{|\nu_0|}} \mathcal{F}(\theta, \phi) \hat{e}_0 \quad (29)$$

$$\hat{q}_1 = \frac{1}{\sqrt{|\nu_1|}} \mathcal{F}(\theta, \phi) \hat{e}_1 \quad (30)$$

$$\hat{q}_0 \cdot \hat{q}_1 = \hat{e}_0^T \mathcal{H} \hat{e}_1 = 0. \quad (31)$$

$$\|\hat{q}_0\| = \|\hat{q}_1\| = 1. \quad (32)$$

Since, \hat{q}_0 and \hat{q}_1 have the same form as the detector responses (c.f. Eq. 4), they are confined to the response plane. Let γ be the angle between $\hat{\mathbf{S}}$ and \hat{q}_0 . Then,

$$\mathbf{S} = \|\mathbf{S}\| (\hat{q}_0 \cos \gamma + \hat{q}_1 \sin \gamma), \quad (33)$$

The SNR variability measure $\Gamma(\theta, \phi; \hat{S})$ then becomes a function $\Gamma(\theta, \phi; \gamma)$ of γ .

Recall Eq. 11 for the definition of the quantity λ that we want to maximize over the response vector \mathbf{S} . We can now rewrite it as,

$$\lambda = (\mathbf{X} \cdot \hat{q}_0) \rho \cos \gamma + (\mathbf{X} \cdot \hat{q}_1) \rho \sin \gamma - \frac{1}{2} \rho^2, \quad (34)$$

where $\rho = \|\mathbf{S}\|$. From the above it is obvious that the solution for \mathbf{S} that maximizes λ is the projection of \mathbf{X} onto the response plane.

V. PENALIZED MAXIMIZATION OF LIKELIHOOD RATIO

We have shown that SNR variability, as measured by $\Gamma(\theta, \phi; \gamma)$ defined in Eq. 28, correlates well with how improbable a solution of the LR maximization problem is. Improbable waveforms $h_+[k]$ and $h_\times[k]$ that lead to very different responses in nearly aligned detectors also correspond to a fast variation in the detectability of the source as it is displaced on the sky. Such sources naturally become rare compared to probable ones. In this Section, we construct a detection statistic that incorporates $\Gamma(\theta, \phi; \gamma)$ to restrict the influence of improbable solutions on the maximization of the LR.

A. Algebraic simplifications

We begin by making some algebraic simplifications. Substituting Eq. 33 into 28, we get,

$$\Gamma^2(\theta, \phi, \gamma) = (\cos \gamma \ \sin \gamma) \mathcal{M} \begin{pmatrix} \cos \gamma \\ \sin \gamma \end{pmatrix}, \quad (35)$$

$$\mathcal{M} = \begin{pmatrix} A & C \\ C & B \end{pmatrix}, \quad (36)$$

$$A = \frac{1}{|\nu_0|} (\|\mathcal{F}_\theta \hat{e}_0\|^2 + \|\mathcal{F}_\phi \hat{e}_0\|^2), \quad (37)$$

$$B = \frac{1}{|\nu_1|} (\|\mathcal{F}_\theta \hat{e}_1\|^2 + \|\mathcal{F}_\phi \hat{e}_1\|^2), \quad (38)$$

$$C = \frac{1}{\sqrt{|\nu_0 \nu_1|}} [(\mathcal{F}_\theta \hat{e}_0) \cdot (\mathcal{F}_\theta \hat{e}_1) + (\mathcal{F}_\phi \hat{e}_0) \cdot (\mathcal{F}_\phi \hat{e}_1)]. \quad (39)$$

We now perform another change of basis in the response plane. Let the eigenvalues and eigenvectors of \mathcal{M} be μ_0 , $\mu_1 \leq \mu_0$ and \hat{m}_0 and \hat{m}_1 respectively. Since \hat{m}_0 and \hat{m}_1 form an orthonormal basis,

$$\begin{pmatrix} \cos \gamma \\ \sin \gamma \end{pmatrix} = \hat{m}_0 \cos \psi + \hat{m}_1 \sin \psi, \quad (40)$$

for some angle ψ between the response vector \mathbf{S} and \hat{m}_0 . Then,

$$\Gamma^2(\theta, \phi; \gamma) = \mu_0 \cos^2 \psi + \mu_1 \sin^2 \psi. \quad (41)$$

Henceforth, we denote $\Gamma^2(\theta, \phi; \gamma)$ as $\Gamma^2(\theta, \phi; \psi)$.

Using the orthonormal basis vectors \hat{m}_0 and \hat{m}_1 , we can state

$$\begin{pmatrix} \mathbf{X} \cdot \hat{q}_0 \\ \mathbf{X} \cdot \hat{q}_1 \end{pmatrix} = \alpha_x \hat{m}_0 + \beta_x \hat{m}_1, \quad (42)$$

where α_x and β_x denote the components along \hat{m}_0 and

\hat{m}_1 respectively. From Eq. 34 and 42, it follows that,

$$\begin{aligned} \lambda &= \rho (\cos \gamma \ \sin \gamma) \begin{pmatrix} \mathbf{X} \cdot \hat{q}_0 \\ \mathbf{X} \cdot \hat{q}_1 \end{pmatrix} - \frac{1}{2} \rho^2, \\ &= \rho (\alpha_x \cos \psi + \beta_x \sin \psi) - \frac{1}{2} \rho^2, \\ &= \rho l_x \cos(\psi - \phi_x) - \frac{1}{2} \rho^2, \end{aligned} \quad (43)$$

$$l_x = \sqrt{\alpha_x^2 + \beta_x^2}, \quad (44)$$

$$\phi_x = \tan^{-1} \left(\frac{\beta_x}{\alpha_x} \right). \quad (45)$$

The maximization of λ has to be performed over ρ and ψ . Thus, the SL solution is $\rho = l_x$, the length of the projection of \mathbf{X} onto the response plane, and $\psi = \phi_x$ which is the angle between the projection and the \hat{m}_0 vector.

B. Penalized maximization

Now we introduce one possible way to incorporate $\Gamma(\theta, \phi, \psi)$ into the maximization of λ . We call this method *penalized maximum likelihood ratio* (PMLR). We propose to maximize λ' ,

$$\lambda' = \lambda - \alpha \Gamma^2(\theta, \phi, \psi), \quad (46)$$

where $\alpha \geq 0$ is a parameter under our control. The extra term $\alpha \Gamma^2(\theta, \phi, \psi)$ acts as a penalty that prevents the solution from readily converging to the data vector \mathbf{X} . This resolves the two detector paradox (c.f., Section III).

Once the solution $\hat{\rho}$, $\hat{\psi}$ that maximizes λ' in Eq. 46 is found, we find the value of λ at this solution (not λ'). Our final data functional will be the sum of the values of λ , found as above, over all samples of the data \mathbf{X} . Reintroducing the time index and denoting the resulting functional as $\Lambda_{\text{PL}}(\theta, \phi)$, we get

$$\Lambda_{\text{PL}}(\theta, \phi) = \sum_j \max_{\rho, \psi} \left[\rho l_x[j] \cos(\psi[j] - \phi_x[j]) - \frac{1}{2} \rho[j]^2 - \alpha (\mu_0 \cos^2 \psi[j] + \mu_1 \sin^2 \psi[j]) \right]. \quad (47)$$

The global maximum of $\Lambda_{\text{PL}}(\theta, \phi)$, over θ and ϕ , will serve as the final detection statistic.

The solution $\hat{\rho}$, $\hat{\psi}$ that maximizes λ' is easily found.

$$\hat{\rho} = l_x \cos(\hat{\psi} - \phi_x), \quad (48)$$

$$\tan(2\hat{\psi}) = \frac{\sin(2\phi_x)}{\cos(2\phi_x) - 2\alpha(\mu_0 - \mu_1)/l_x^2}. \quad (49)$$

Note that when $\alpha = 0$, we recover the standard likelihood ratio statistic $\Lambda_{\text{SL}}(\theta, \phi)$ wherein the solution for \mathbf{S} is the

data \mathbf{X} projected on the 2D response plane. Also, the importance of the penalty term diminishes as l_x^{-2} . If a signal is present, the latter increases with an increase in the instantaneous signal amplitude. Hence, whenever the signal amplitude is strong enough, the effect of the penalty term is reduced at that instant and the wave form estimators $\hat{\psi}$ and $\hat{\rho}$ converge to the SL estimates.

The term $\mu_0 - \mu_1$, which is always positive by definition, is a measure of how misaligned the detectors in a network are. This difference is reduced with an increase

in misalignment, hence reducing the effect of the penalty term. Fig. 3 shows $\mu_0 - \mu_1$ as a function of sky position for two networks: (1) three LIGO detectors: one at Livingston, and two at Hanford, and (2) one LIGO detector at Livingston, one GEO600 and one VIRGO detector. Fig 3 also shows the ratio of the differences in eigenvalues for the two networks. It is clear that the difference in eigenvalues for the first network, which consists of nearly aligned detectors, is larger than that for the second network over a large fraction of the sky.

The statistic $\Lambda_{\text{PL}}(\theta, \phi)$ solves the two detector paradox by continuously bridging the aligned and misaligned detectors cases. From Eq. 49, it is clear that as $\mu_0 - \mu_1$ increases, i.e., as the detectors become more aligned, the denominator increases in the negative direction while the numerator, $\sin 2\phi_x$, stays the same. Hence, $2\psi \rightarrow \pi$ which implies $\psi \rightarrow \pi/2$. From Eq. 41, the penalty function Γ^2 has its lowest value for $\psi = \pi/2$. This is the direction in the response plane along which all the responses in a network get oriented as the detectors are aligned. Therefore, with progressive alignment of the detectors in a network, the solution $\hat{\psi}$ is forced towards equal responses in all detectors, thus leading smoothly into the completely aligned case. In contrast, for the standard likelihood statistic $\Lambda_{\text{SL}}(\theta, \phi)$ ($= \Lambda_{\text{PL}}$ when $\alpha = 0$), there exists a fundamental discontinuity between the solutions for aligned and misaligned cases: For the aligned case $\hat{\psi} = \pi/2$, while $\hat{\psi} = \phi_x$ for the misaligned case.

Finally, the penalty term, Γ^2 , depends only the direction of the instantaneous network response vector \mathbf{S} . It does not restrict its length. Hence, the magnitude of \mathbf{S} at two distinct time instants can be arbitrarily different. Thus, even white noise response waveforms are allowed as solutions. The only requirement is on the mutual consistency of detector responses at each instant of time.

C. Connection with Bayesian analysis

The penalized likelihood approach, Eq. 46, has a straightforward connection to Bayesian [18] analysis. In the latter approach, the posterior degree of belief over the space of waveforms, or equivalently ρ and ψ (c.f., Eq. ref), is obtained using Bayes' law,

$$p(\rho, \psi | \mathbf{X}) = \frac{p(\rho, \psi)p(\mathbf{X} | \rho, \psi)}{p(\mathbf{X})}, \quad (50)$$

where $p(\mathbf{X} | \rho, \psi)$ is simply the likelihood λ in Eq. 11. The maximum a posteriori Bayesian estimates for the true ρ and ψ would be the ones for which $p(\rho, \psi | \mathbf{X})$ is maximized. This is equivalent to maximizing the logarithm of $p(\rho, \psi | \mathbf{X})$ and, hence, the sum of λ and $\log p(\rho, \psi)$. Comparison with Eq. 46 shows that $1/\Gamma^2$ acts as a prior. The difference is that this prior is not normalized in Eq. 46 but is instead multiplied by α . Of course, α can be chosen to be the integral of $1/\Gamma^2$ over ψ thus reducing the penalized maximization to a true Bayesian analysis.

VI. RESULTS

The PMLR method was implemented in Matlab [24] and its performance was quantified with the Monte Carlo simulation code previously used in [15]. We give a brief recapitulation of the simulation scheme: Binary Black Hole merger waveforms from [25] are injected into short stretches of white noise, one waveform per stretch. The signals correspond to face-on binaries scattered uniformly on the sky with randomly selected polarization angles. The signals have a variable matched filtering SNR due to their sky position and polarization, but an overall factor G is used to scale the amplitudes of the two polarizations $h_+(t)$ and $h_\times(t)$. The sky-averaged SNR of the injected signals is approximately related to G as $SNR \simeq 2.3G$. Further details can be found in [15].

Consider, first, some case studies to give a qualitative feel for the performance of PMLR compared to the SL and constraint likelihood methods. Fig 4 compares SL, constraint likelihood (hard constraint) and PMLR (with $\alpha = 1500$) for the same signal using the three detector network: Hanford, Livingston and GEO. The true sky position of the source was $\theta = 50^\circ$, $\phi = 280^\circ$. The best estimates for sky position (in degrees) were (1) $\theta = 76^\circ$, $\phi = 32^\circ$ for SL and (2) $\theta = 48^\circ$, $\phi = 280^\circ$ for PMLR and constraint likelihood. Note that, compared to SL, the sky maps for constraint likelihood and PMLR are less noisy and show more contrast between the region in which the signal is located and the rest of the sky.

The simulation code finds out the fraction of all injected binaries detected by the PMLR (or other) method. The detection statistic for all methods is the maximum value over the respective skymap (e.g. Fig 4). Fig 5 shows the receiver operating characteristics (ROC) for SL, constraint likelihood (both hard and soft constraint) and PMLR (with $\alpha = 150$ and 1500). The measured fraction of detected signals is plotted against the false alarm rate corresponding to the detection threshold used. It is clear from the figure that PMLR can vary continuously in performance, ranging from SL for low values of α to the hard constraint method for high values.

The simulation code also estimates the error in sky position reconstruction. Fig. 6 shows the fraction of the injected signals that were detected within 8 degrees of their true position, for a range of the scale factor G . The PMLR method ($\alpha = 1500$) has practically the same performance as the hard constraint method and both perform somewhat better than the soft constraint method. The performance of SL, however, is significantly worse than all the other methods. This can also be seen qualitatively in the sky maps of the various methods (Fig. 4) where the SL sky map always has less ‘‘contrast’’ around the true signal location compared to the constraint likelihood and PMLR methods.

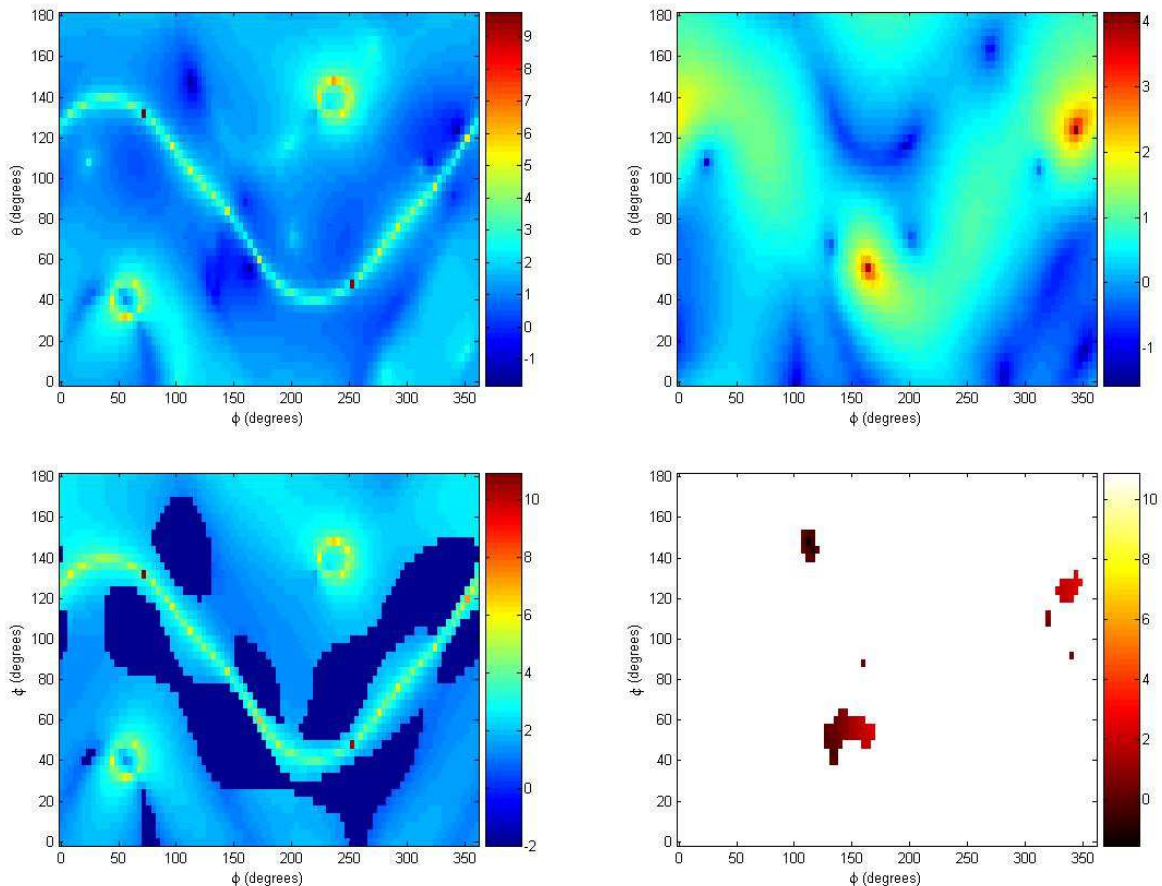


FIG. 3: The difference in eigenvalues μ_0 and μ_1 plotted as a function of sky-position angles θ and ϕ . (All panels display the logarithm to base 10 of $\mu_0 - \mu_1$.) The top left panel is for a network consisting of three LIGO detectors: two at Hanford and one at Livingston. The top right panel is for a network consisting of one LIGO detector at Livingston, one GEO and one VIRGO detector. The first network (top left), which is more aligned, shows much larger values of $\mu_0 - \mu_1$ than the second (top right) which has more misalignment between the detectors. In the bottom left panel, the part of the sky where $\mu_0 - \mu_1$ for the first network is ≤ 10 times that for the second network has been suppressed. It is clear that this is a smaller fraction of the sky compared to the part where $\mu_0 - \mu_1$ for the first network is ≥ 10 times that of the second network. In the bottom right panel, only the part of the sky where $\mu_0 - \mu_1$ for the second network is greater than or equal to that for the first network is shown.

VII. CONCLUSION

There exists a serious problem, called the two detector paradox, in the formal application of the standard likelihood method to the detection of burst GW signals. We resolve this problem by imposing a restriction on the detector responses allowed as candidate solutions for maximizing the likelihood functional. The restriction is imposed through a penalizing function that measures the variability of the SNR of a candidate solution when the corresponding source is displaced slightly on the sky. High SNR variability sources lead to very different detector responses even when the detectors are closely aligned. The standard likelihood method allows such sources as perfectly valid candidate solutions. However, such abnormal sources have an inherently reduced observability. The proposed method (PMLR) sacrifices the detectability of such sources while boosting the sensitivity and

sky position reconstruction accuracy for normal signals.

PMLR contains a free parameter, the penalty factor α . For $\alpha = 0$ PMLR simply reduces to the SL method. However, method is not very sensitive to the exact value of α , and the sky map of the likelihood converges rapidly as α is made large. The role of α needs to be investigated further.

Results from numerical simulations show that the performance of the PMLR method can be tuned, using α , to vary over the range covered by the standard likelihood and the constraint likelihood methods introduced in KMRM. For the type of source population used in the simulations, a high value of α yields the same performance as the hard constraint method. The ROC curves are mildly better compared to standard likelihood but the accuracy of source direction reconstruction is significantly better.

PMLR is also related to the Bayesian approach. Work

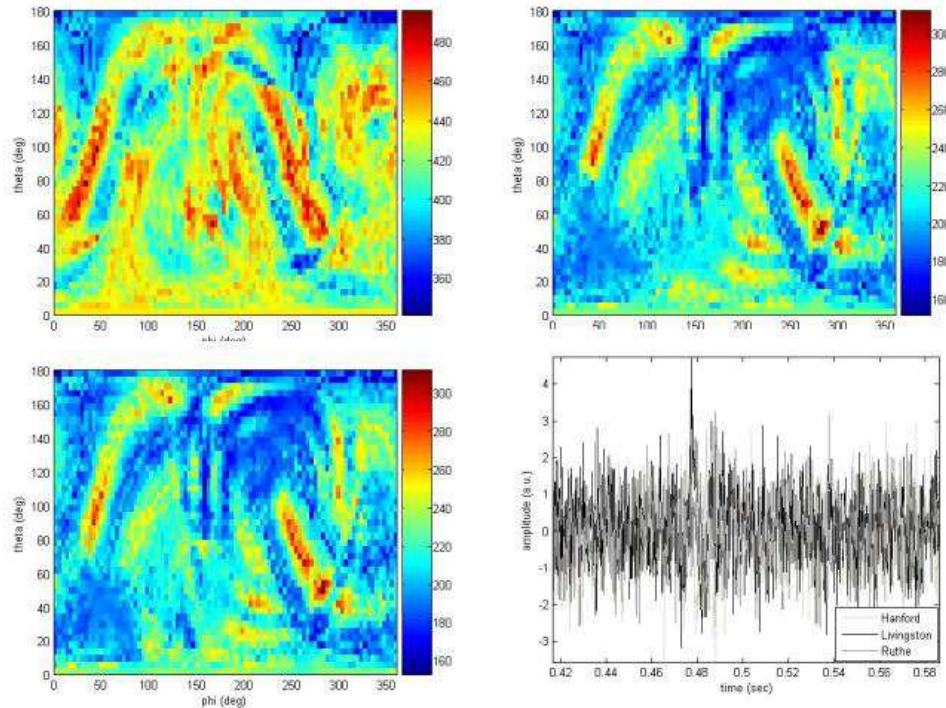


FIG. 4: Comparison of SL (top left), constraint likelihood (hard constraint) (top right) and PMLR (bottom left) for $\alpha = 1500$. The source is at $\theta = 50^\circ$, $\phi = 280^\circ$ and has an amplitude scale factor of $G = 3$. The network consists of one detector at Hanford, one at Livingston and GEO. The detector responses, assuming white Gaussian noise, are shown in the bottom right panel.

in the latter direction has focussed on using priors that suppress candidate solutions that are not smooth. (This is equivalent to the requirement that the signals have a smaller frequency bandwidth than the noise.) However, the penalty in PMLR is not based on the smoothness of signals in time. It is on signals that lead to widely different responses in nearly aligned detectors. In particular, a white noise burst signal is perfectly admissible as a candidate solution in PMLR. If smoothness constraints are desired, they can be added on to the PMLR restriction.

The approach introduced in this paper can be extended to include variability of observed SNR as a function of source inclination to line of sight and the projected orientation of the source on the sky. This extension may result in a penalizing function with better performance than the one used in this paper.

Acknowledgments

We thank an anonymous referee from the LIGO Science Collaboration for useful comments on the text. This work was supported by the US National Science Foundation grants PHY-0244902, PHY-0070854 to the University of Florida, Gainesville and NASA grant NAG5-13396 to the Center for Gravitational Wave Astronomy at the University of Texas at Brownsville. M.R. was supported by NSF awards PHYS 02-44902, PHYS 03-26281 and the NSF Center for Gravitational Wave Physics. The Center for Gravitational Wave Physics is funded by the National Science Foundation under cooperative agreement PHY-01-14375.

[1] A. Abramovici *et al.*, *Science* **256** 325-333 (1992).
 [2] F. Acernese *et al.*, *Class. Quantum Grav.* **21**, S385 (2004).
 [3] B. Willke *et al.*, *Class. Quantum Grav.* **21**, S417 (2004).
 [4] M. Ando and the TAMA collaboration, *Class. Quantum Grav.* **19**, 1409 (2002).

[5] IGEC: International Gravitational wave Event Collaboration, <http://igec.lnl.infn.it/>
 [6] A. Stuart, K. Ord, *Kendall's Advanced Theory of Statistics*, Vol.2, 5th Edition (Edward Arnold, 1991).
 [7] L. S. Finn, *Phys. Rev. D* **63**, 102001 (2001).
 [8] A. Pai, S. Dhurandhar, S. Bose, *Phys. Rev. D* **64**, 042004

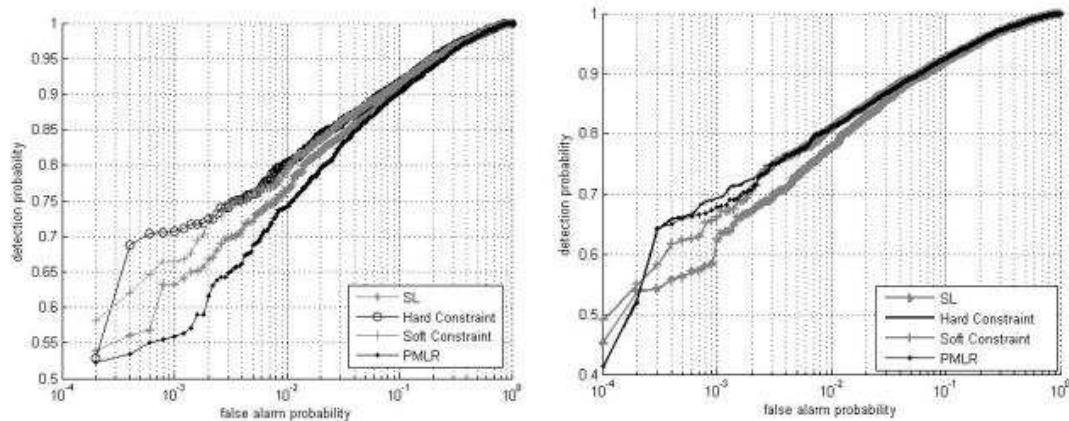


FIG. 5: Receiver Operating Characteristics for SL, constraint likelihood (both hard and soft constraint) and PMLR. The value of the penalty factor $\alpha = 150$ and $\alpha = 1500$ for the left and right panels respectively. The number of trials was 5000 for both the left and right plots. The signal amplitude factor for this simulation was $G = 3.0$ which corresponds to an average SNR of ≈ 7.0 . The network chosen was one detector at Hanford, one at Livingston and one GEO detector.

- (2001).
- [9] Kimberly C.B. New, “Gravitational Waves from Gravitational Collapse”, *Living Rev. Relativity* **6**, (2003), 2. URL (cited on June 16, 2005): <http://www.livingreviews.org/lrr-2003-2>.
- [10] S. Kobayashi, P. Mészáros, *Astrophys. J.* **589**, 861 (2003).
- [11] É. Flanagan, S. A. Hughes, *Phys. Rev. D* **57**, 4535 (1998).
- [12] É. Flanagan, S. A. Hughes, *Phys. Rev. D* **57**, 4566 (1998).
- [13] S. Mohanty *et al*, *Class. Quantum Grav.* **21**, S1831 (2004).
- [14] Wm. R. Johnston, M.S. thesis, The University of Texas at Brownsville, 2004.
- [15] S. Klimenko *et al*, *Phys. Rev. D* **72**, 122002 (2005).
- [16] Y. Gürsel, M. Tinto, *Phys. Rev. D* **40**, 3884 (1989).
- [17] J. Sylvestre, *Phys. Rev. D* **68**, 102005 (2003).
- [18] A. O’Hagan, J. Forster, *Kendall’s Advanced Theory of Statistics, Vol. 2B: Bayesian Inference*, (Arnold, London, 2004).
- [19] W. Anderson *et al*, *Phys. Rev. D* **63**, 042003 (2001).
- [20] P. R. Brady, S. Ray-Majumder, *Class. Quantum Grav.* **21**, S1839 (2004).
- [21] C. Misner, K. Thorne, J. Wheeler, *Gravitation*, (Freeman, San Francisco, 1973) Chap. 38 .
- [22] S. Dhurandhar and M. Tinto, *Mon. Not. R. Astr. Soc.* **234**, 663 (1988).
- [23] C. W. Helstrom, *Statistical Theory of Signal Detection*, 2nd ed. (Pergamon press, London, 1968).
- [24] Matlab, URL: <http://www.mathworks.com>.
- [25] J. Baker *et al*, *Phys. Rev. D* **65**, 124012 (2002).

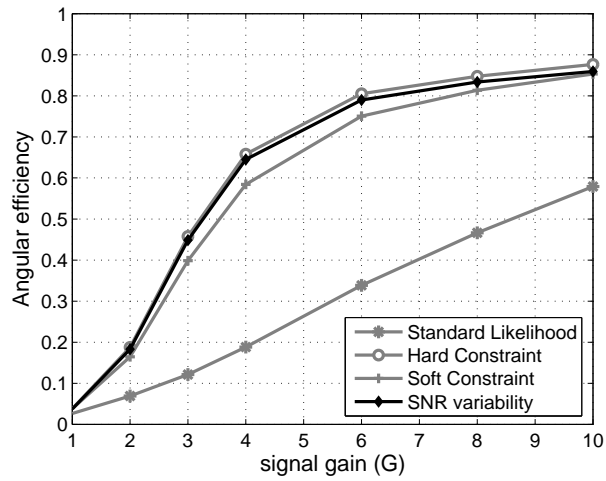


FIG. 6: The fraction of signals detected within 8° of their true positions. As the signal SNR decreases, all methods lose both detection efficiency and incur large errors in direction estimation. At the same time, as the SNR increases, all methods converge to the true signal location in almost all cases. The difference between the methods is, therefore, maximum for intermediated SNRs.